Systematics of isotopic production cross sections from interactions of relativistic ^{40}Ca in hydrogen

C.-X. Chen,[1,*] S. Albergo,[2] Z. Caccia,[2] S. Costa,[2] H. J. Crawford,[3] M. Cronqvist,[3] J. Engelage,[3] L. Greiner,[3] T. G. Guzik,[1] A. Insolia,[2] C. N. Knott,[4] P. J. Lindstrom,[5] M. McMahon,[1] J. W. Mitchell,[6] R. Potenza,[2] G. V. Russo,[2] A. Soutoul,[7] O. Testard,[7] C. E. Tull,[5] C. Tuvé,[2] C. J. Waddington,[4] W. R. Webber,[8] and J. P. Wefel[1]
(The Transport Collaboration)
[1]*Department of Physics and Astronomy, Louisiana State University, Baton Rouge, Louisiana 70803*
[2]*Dipartimento di Fisica, Universitá di Catania and Istituto Nazionale di Fisica Nucleare, Sezione di Catania, Corso Italia 57, I 95129, Catania, Italy*
[3]*Space Science Laboratory, University of California, Berkeley, California 94720*
[4]*School of Physics and Astronomy, University of Minnesota, Minneapolis, Minnesota 55455*
[5]*Lawrence Berkeley National Laboratory, 1 Cyclotron Road, Berkeley, California 94720*
[6]*NASA/Goddard Space Flight Center, Greenbelt, Maryland 20771*
[7]*Service d'Astrophysique, Centre d'Etudes de Saclay, 91191 Gif-sur-Yvette, Cedex, France*
[8]*Department of Astronomy, New Mexico State University, Las Cruces, New Mexico 88003*
(Received 16 April 1997)

The isotopic production cross sections for ^{40}Ca projectiles at 357, 565, and 763 MeV/nucleon interacting in a liquid hydrogen target have been measured by the Transport Collaboration at the LBL HISS facility. The systematics of these cross sections are studied, and the results indicate that nuclear structure effects are present in the isotope production process during the relativistic collisions. The newly measured cross sections are also compared with those predicted by semiempirical and parametric formulas, but the predictions do not fully describe the systematics such as the energy dependence. The consequences of the cross section systematics in galactic cosmic ray studies are also discussed. [S0556-2813(97)04809-7]

PACS number(s): 25.75.−q, 26.40.+r, 25.70.Lm, 98.70.Sa

I. INTRODUCTION

The near-Earth measurements of galactic cosmic ray (GCR) isotopic abundances and energy spectra can provide key information regarding GCR source(s), particle acceleration and deceleration mechanisms, and the effect of propagation through the interstellar medium [1–3]. However, the energy and composition changes that occur during the transport of cosmic ray particles must be accounted for during such studies. A number of processes contribute to these changes, but by far the most important parameters necessary to interpret GCR measurements are those due to nuclear fragmentation and the consequent energy-dependent production cross sections in the interstellar medium (ISM) [4]. In fact, for some cases, accurate propagation calculations may require a very precise knowledge of the isotopic production cross sections, along with charge- and mass-changing partial and total reaction cross sections. With limited accelerator data on such fragmentation processes [5–10], predictive formulas based upon existing data become a necessity [11–15]. However, the algorithms used in these prediction codes may not be reliable for unmeasured reactions and can only be constrained by additional measurements. Thus some key interactions must be studied, not only for the cross section values themselves, but also for a better understanding of the cross section systematics, which can be used to improve the accuracy of cross section predictions.

As one of the key elements during stellar evolution, and also a major link between heavy and medium GCR components, calcium plays an important role in various astrophysical processes. Although gas-phase calcium is highly depleted [16], the overall abundance of calcium in GCR is enhanced above the normal solar system composition by a factor of 3–4 [1]. This is mostly due to the spallation of heavier GCR nuclei, such as the iron-nickel group, with the interstellar medium. Different isotopes of calcium are the progenies of different nucleosynthetic processes [17–22]. Also, ^{40}Ca can fragment into lighter species and therefore contribute to various measured GCR components such as chlorine, sulfur, silicon, magnesium, and neon. The GCR source ratios of ^{34}S/^{32}S, ^{30}Si/^{28}Si, ^{29}Si/^{28}Si, and ^{22}Ne/^{20}Ne are among the key differences separating various GCR origin models [1–3]. Since the source ratios are derived from near-Earth measurements, a significant portion of their uncertainties are from the nuclear cross sections used in the GCR propagation calculations. For example, the GCR source ^{22}Ne/^{20}Ne ratio, currently determined to be 5 times larger than the normal solar system composition, is the most important as well as the unique feature of the Wolf-Rayet model, which also predicts the relative abundances of other GCR source isotopes. A case study made recently by the Transport Collaboration for the ^{18}O enhancement using the new ^{22}Ne and ^{26}Mg cross section data [7] showed that the ^{18}O abundance can vary widely if cross sections predictions are used, but is consistent with solar system composition if measured cross sections are used.

For the nuclear interaction systematics calcium has particular, interesting properties. It is the only element in the

*Current address: Horizon Computers, Inc., 5 Lincoln Highway Edison, New Jersey 08820.

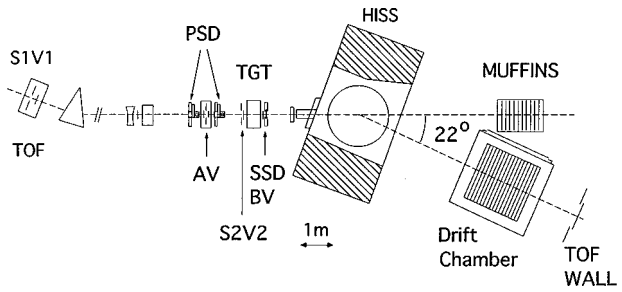

FIG. 1. Schematic diagram of the experimental setup at the LBL HISS facility.

beta-stable nuclear structure that has two doubly magic isotopes, with two neutron shells ($1d_{3/2}$, $1f_{7/2}$) successively filled from ^{40}Ca to ^{48}Ca alongside the closed proton $1d_{3/2}$ shell. Because of such a key position in the chart of nucleides, there is intense theoretical and experimental interest in studying calcium, including topics such as nuclear equation-of-state, shell model, nuclear charge distribution and radii, isotope shift, etc. [23–27]. Nuclear structure such as that of calcium has important effects on nuclear interaction systematics. Previous investigations of heavy ion fragmentation at relativistic energies have shown that the process can be influenced by various nuclear effects such as shell structure and nucleus isospin [7,8]. Therefore, the individual isotopic production cross sections contain the signatures of the fragmenting nuclei as part of their systematics.

To address issues such as these, the Transport Collaboration initiated a program to measure the projectile fragmentation cross sections for heavy ions ($Z \geqslant 2$) in a liquid hydrogen target [28]. In April 1990 and April 1991, the collaboration obtained data for 20 projectile-energy combinations [29–31] using the Lawrence Berkeley Laboratory (LBL) Bevalac Heavy Ion Spectrometer System (HISS) facility and a liquid hydrogen target. In this paper we present the measurement of isotopic production cross section results of ^{40}Ca nuclei of 357, 565, and 763 MeV/nucleon interacting in a liquid hydrogen target. We also investigate the cross section systematics, compare the results with other projectile species, and look at the predictions of the semiempirical and the parametric cross section models.

II. EXPERIMENT

The experimental apparatus used at LBL to measure the nuclear interaction cross sections, illustrated in Fig. 1, is designed to identify fragment isotopic masses (A) using the charge-velocity-rigidity technique with the formula

$$A = \frac{RZec}{\beta\gamma m_N c^2}, \tag{1}$$

where R is the fragment rigidity, Z is the charge, β is the reduced velocity, γ is the Lorentz factor, and m_N is the nucleon mass. The full experimental setup includes six primary subsystems: the beam detection system, which includes the beam geometry definition scintillators (S1V1, AV, S2V2) and position-sensitive detectors (PSDs), liquid hydrogen target (TGT) with post-target charge detectors (SSD, BV), HISS (Heavy Ion Spectrometer System) magnet, drift chamber (DC), time-of-flight (TOF) wall, and neutron detector (MUFFINS). One of the features in the setup is the specially designed liquid hydrogen target, in which the interaction between the projectile and a proton takes place. Although such a target is difficult to operate and calibrate, it provides a direct measurement of heavy ions, on proton interactions, mimicking the propagation effects of GCR through the ISM, which is at least 90% hydrogen. Further details of the experiment configuration, detectors, and liquid hydrogen target can be found in Refs. [29–31].

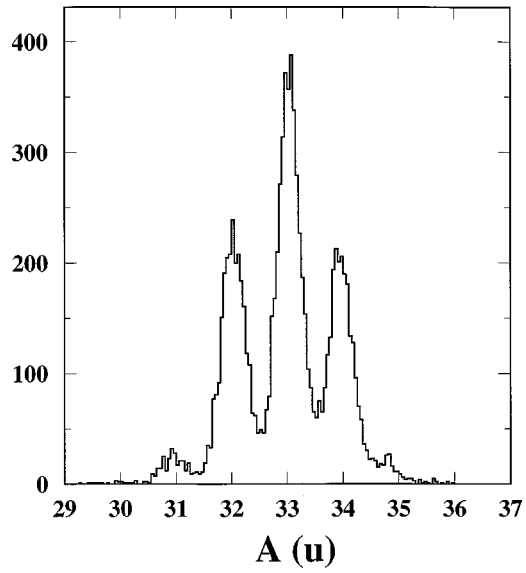

FIG. 2. Mass histogram for ^{40}Ca+H$\rightarrow_{16}$S at 565 MeV/nucleon.

The isotopic production analysis was performed using the ''pseudorigidity'' and ''pseudomass'' technique described in detail in Ref. [7]. Basically, we applied the first order relationship between the fragment rigidity and its track-bending angle as well as time of flight to obtain the isotope mass separation required for the analysis. Figure 2 shows a mass histogram for sulfur isotopes from ^{40}Ca+H at 565 MeV/nucleon. The overall mass resolution obtained using this technique is 0.15–0.35 u over the range of data reported.

The isotopic production cross section is first calculated using the ''thin target'' approximation

$$\sigma(Z,A) = \frac{1}{t}\frac{N(Z,A)}{N_{\text{total}}}, \tag{2}$$

where

$$t = \frac{(N_A L)\times 10^{-27}}{A_H}\ (\text{mb}^{-1}) \tag{3}$$

is the effective hydrogen target thickness, N_A is Avogadro's number, L is the hydrogen depth in g/cm^2, and A_H is the hydrogen atomic weight. The isotopic population $N(Z,A)$ is the yield of a particular isotope resulting from interactions in the target. N_{total} is the total incoming projectile population.

Determining final numbers for N_{total} and $N(Z,A)$ involves various corrections and normalizations, and a final ''thick target'' adjustment. The various sources which contribute to the final cross section uncertainties are statistics, fitting, effective target thickness, ''target-out'' background subtrac-

tion, trigger normalization, acceptances and efficiencies, charge consistency cuts, and thick target calculations. The details of the data and uncertainty analysis are described in Refs. [7,8]. The final isotopic production cross sections for ^{40}Ca+H at three energies using the entire data set are listed in Table I.

III. CROSS SECTION SYSTEMATICS

In Fig. 3 we plot all the new cross sections, element by element. In general, the isotopic cross sections for the different energies have a quite similar mass dependence with only small differences for the rare neutron poor fragments. Yet some of the individual yields are significantly energy dependent. This is revealed by broadening of the distributions, seen especially in large charge-change (ΔZ) fragments. For fragments with small ΔZ down to phosphorus, the energy dependence is minimal. However, for large ΔZ fragments such as silicon and lighter, the effect of projectile energy starts to be observed. The energy dependence becomes very pronounced for magnesium, sodium, and neon. This indicates, not surprisingly, that there is more disruption of the nuclei occurring at higher energies. The overall charge-changing total cross sections and partial elemental cross sections published earlier [8,29] pointed to a similar energy dependence.

A recent analysis of the neutron production from the same ^{40}Ca projectiles at 357 and 565 MeV/nucleon has yielded an even stronger energy dependence than seen here for the isotope production [32]. The total neutron production cross section more than doubles from 357 to 565 MeV/nucleon, while the total charge-changing cross section only increases by ~10% [29]. It is not clear why many more neutrons are produced, except that more disruptive collisions increase the possibility for breaking nuclei up into more small fragments.

The mass distributions for each element have their own interesting characteristics. For lighter projectiles such as sulfur, the isotopic mass distribution is always centered at the same isospin, or Z/A ratio, as the projectile and shows a Gaussian type of shape [9]. However, the fragmentation process for calcium favors neutron-rich isotope production, although ^{40}Ca itself is balanced. Another feature is that for odd-Z fragments, such as potassium, chlorine, phosphorus, aluminum, and sodium, there is a dominant isotope whose isospin differs from the projectile's by 1/2. Among these dominant channels, the large cross section values are for the fragments with spin-parity state $J^{\pi}=\frac{3}{2}^{+}$, while ^{40}Ca itself has $J^{\pi}=0^{+}$. It seems that the Coulomb repulsion effect in the nuclear structure of the projectile is manifest in the interaction process. One possible scenario may be that during the final evaporation phase of the interaction, the Coulomb repulsion from the original nucleus tends to eject protons over neutrons.

The one-neutron stripping cross sections are very comparable (to within 30%–50%) with those of one-proton stripping. This may indicate that both the outermost neutron and the outermost proton have similar spatial orbits. However, the two-proton stripping cross sections are very significant compared to the almost nonexistent two-neutron stripping process. Recent measurements on ^{36}Ar ^{40}Ar projectiles by the Transport Collaboration [10] using the same experimental apparatus have demonstrated that ^{36}Ar also has a large two-proton stripping cross section, whereas ^{40}Ar does not. It appears that these large cross sections are only present for nuclei with $N=Z$. Again, it is possible that this reflects the neutron and proton radial distributions within the nucleus.

The ^{40}Ar measurements were made at an energy of 352 MeV/nucleon and hence can be compared directly with the low energy ^{40}Ca results. This allows us to make comparisons between two projectiles with the same mass, but different nuclear structures, with minimum influence from experiment differences. Figure 4 shows the isotopic production cross sections from the two projectiles as functions of ΔN (number of neutron change), grouped in ΔZ (number of proton change). For individual ΔZ channels, each projectile has its own fragment mass distribution usually centered on a peak ΔN. One striking feature is that no matter how much charge changing (ΔZ) has happened to the nuclei, there is consistently a ΔN of 3–4 between the ^{40}Ar and ^{40}Ca distribution peaks. This indicates that the four extra neutrons added to ^{36}Ar to form the ^{40}Ar nucleus are less tightly bound then the same four neutrons included in the closed shell of the ^{40}Ca nucleus.

To further demonstrate this observation, Fig. 5 shows the magnitude of the isotopic production cross section as a function of the neutron number (N) and the proton number (Z), along with the total mass ($A=N+Z$) and the isospin number ($T_Z=A/2-Z$), for both ^{40}Ca [panel (a)] and ^{40}Ar [panel (b)]. The size of the open circle represents the magnitude of the cross section, where a diameter of one N (or Z) unit is 50 mb. Open squares are the stable nuclei, and the crosshatching marks the uninteracted projectile species. The distributions of fragments from ^{40}Ca projectiles tend to be centered around neutron-rich $T_Z=+1/2$, while those fragments from ^{40}Ar projectiles are centered around $T_Z=+1$. Other systematics such as the even-odd behavior at $T_Z=0$ and $T_Z=1$ are discussed in detail in the context of the Transport Collaboration ^{36}Ar and ^{40}Ar measurements [10]. It is feasible that in the case of ^{40}Ar-^{40}Ca comparison, the excess neutrons in ^{40}Ar require less disruptive collisions to be knocked off, resulting large neutron-rich fragment production.

IV. COMPARISONS WITH PREDICTIONS

For GCR propagation studies, two widely adopted techniques for predicting isotopic production cross sections are the Silberberg-Tsao semiempirical formulas [12] and the Webber-Kish-Schrier parametric calculation [15]. Both of these techniques use analytic expressions with adjustable parameters to mimic the systematics preceived in a data set of cross sections measurements. The assumption is, then, that these analytic expressions reflect the cross section systematics globally and can be used to predict unmeasured values. Thus it is important to compare the new cross section measurements of this work with values from the predictive formulas. Because of the amount of data involved, we choose a few examples for these comparisons that are significant, either in the magnitude of the cross section or for astrophysics reasons.

The cross sections for particular even-Z fragments as a function of energy are shown in Fig. 6, while selected odd- z fragments are plotted in Fig. 7. The solid curves in both

TABLE I. Isotopic production cross sections from ^{40}Ca on a hydrogen target.

		356 MeV/nucleon		565 MeV/nucleon		763 MeV/nucleon	
Z	A	σ (mb)	$\Delta\sigma$ (mb)	σ (mb)	$\Delta\sigma$ (mb)	σ (mb)	$\Delta\sigma$ (mb)
20	39	25.6	13.2	34.4	7.7	29.8	6.4
							+1.0
20	38	0.0	+1.7	1.3	0.9	0.3	−0.3
19	39	38.9	10.9	39.6	7.2	54.7	7.9
19	38	21.6	9.0	23.2	5.8	21.1	8.6
19	37	12.0	2.3	5.3	1.0	4.6	1.9
					+0.2		+0.4
19	36	0.0	+0.6	0.1	−0.1	0.1	−0.1
18	38	18.6	2.4	23.0	1.6	19.4	2.0
18	37	50.2	3.9	43.7	2.2	44.3	3.6
18	36	31.6	3.1	28.8	1.7	33.6	3.3
18	35	8.1	0.9	4.6	0.5	4.8	0.7
18	34	0.4	0.2	0.3	0.1	0.3	0.2
17	37	2.1	0.4	2.6	0.2	2.7	0.4
17	36	8.6	1.3	12.1	0.9	11.7	1.3
17	35	36.9	3.3	29.9	1.7	33.6	2.3
17	34	16.3	1.6	14.6	1.1	15.2	1.5
17	33	2.9	0.5	1.3	0.2	1.4	0.4
17	32			0.2	0.1	0.2	0.1
16	35	1.4	0.3	1.5	0.3	1.3	0.4
16	34	22.2	1.7	20.4	1.1	20.4	1.8
16	33	34.9	2.3	35.7	1.7	36.2	2.4
16	32	24.7	1.9	23.2	1.3	21.2	1.6
16	31	3.8	0.6	2.7	0.3	2.9	0.6
16	30	0.3	0.1	0.2	0.1	0.2	0.1
15	33	1.2	0.3	1.8	0.2	1.3	0.3
15	32	8.0	0.9	9.2	0.7	12.9	1.2
15	31	24.4	2.1	25.4	1.4	24.1	1.9
15	30	10.0	1.2	11.3	0.8	11.7	1.1
15	29	2.3	0.4	0.8	0.2	0.9	0.3
14	31	0.4	0.2	1.2	0.2	0.6	0.3
14	30	9.6	1.0	14.2	0.9	16.7	1.5
14	29	20.4	1.6	24.2	1.4	23.2	2.1
14	28	19.9	1.6	22.5	1.4	27.5	1.9
14	27	1.5	0.3	1.8	0.3	2.6	0.4
13	29	1.1	0.3	0.5	0.1	1.0	0.2
13	28	3.6	0.6	5.0	0.5	5.5	0.6
13	27	13.4	1.6	18.1	1.2	21.2	1.9
13	26	6.3	1.0	8.2	0.7	8.4	0.8
13	25	0.5	0.2	0.7	0.1	0.9	0.2
13	24	0.3	0.1	0.1	0.1	0.1	0.1
12	27	0.5	0.2	0.4	0.3	0.7	0.2
12	26	4.2	0.6	6.4	0.7	6.9	0.7
12	25	5.9	0.9	10.7	1.0	13.4	1.2
12	24	7.2	1.1	11.7	1.0	14.5	1.3
12	23	0.0	+0.3	0.8	0.2	2.1	0.3
11	25	0.0	+0.1	0.3	0.1	0.6	0.2
11	24	0.5	0.4	1.7	0.3	2.5	0.4
11	23	2.9	1.2	7.5	0.7	10.1	1.1
11	22	2.0	0.7	4.1	0.5	5.9	0.8
11	21	0.5	0.3	0.3	0.1	1.0	0.3
10	23	0.0	+0.1	0.1	0.1	0.2	0.1
10	22	0.9	0.4	2.2	0.3	3.4	0.5
10	21	2.2	0.7	5.0	0.6	4.9	0.7
10	20	2.4	0.7	4.2	0.5	5.4	0.8
10	19	0.4	0.2	0.4	0.1	0.6	0.2

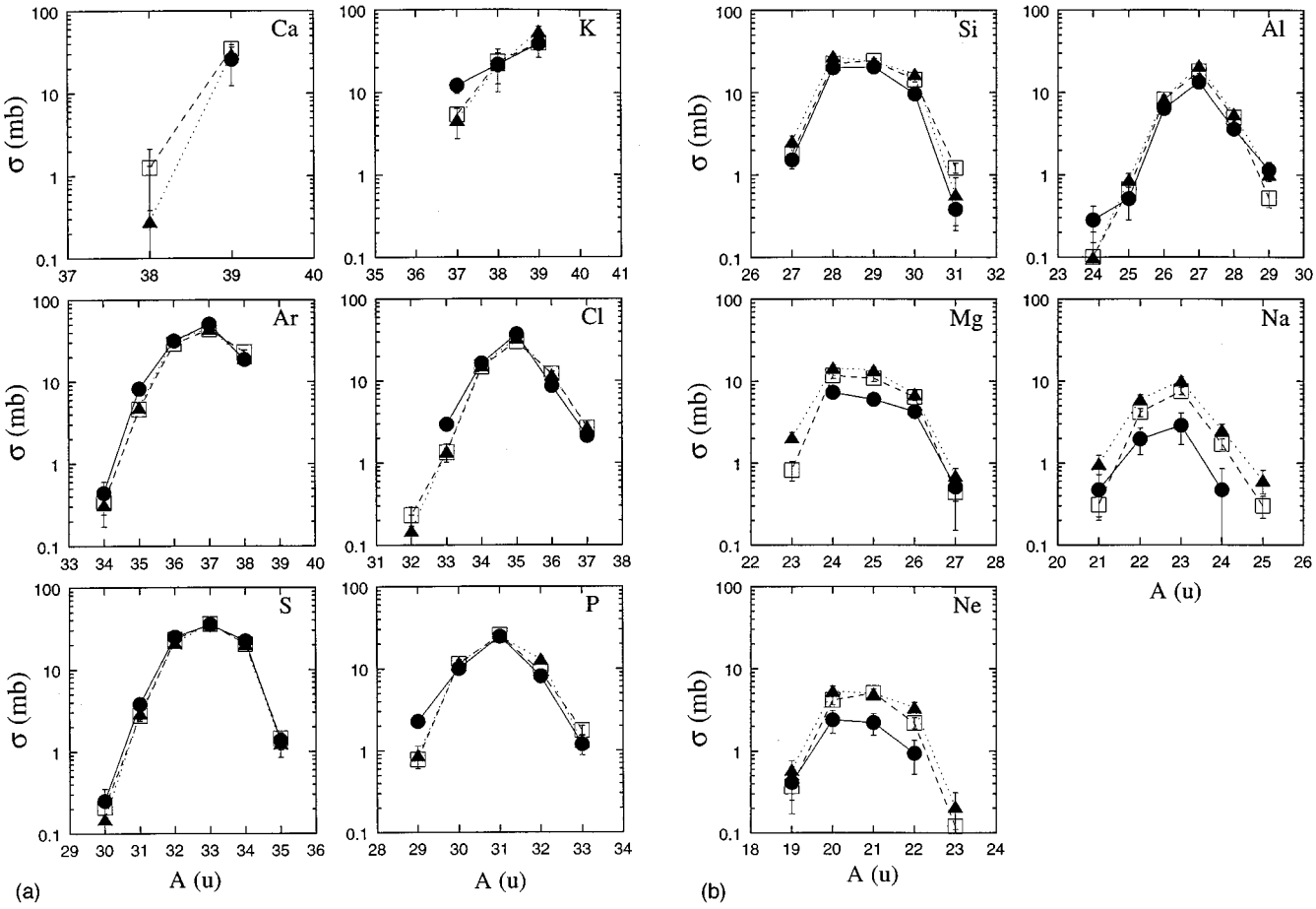

FIG. 3. Isotopic production cross sections for ^{40}Ca+H at three energies. Solid circles are 357 MeV/nucleon data, open squares are 565 MeV/nucleon data, and solid triangles are 763 MeV/nucleon data.

figures are the energy dependence predicted by the semiempirical formulas, and the dashed curves are from the parametric calculations. Also plotted as the open squares are the previous measurements of ^{40}Ca projectiles at 600 MeV/nucleon by Webber, Kish, and Schrier [6], which were used, in part, to develop the parametric calculation technique. For the six isotopes where the earlier measurements are compared to the present results ^{35}Cl, ^{34}S, and ^{30}Si are in agreement while the new data for ^{32}S, ^{31}P, and ^{28}Si are above the previous work. It is difficult to reconcile the S and Si measurements, since a normalization offset that would bring ^{28}Si and ^{32}S into agreement would force ^{30}Si and ^{34}S into disagreement. We have looked at the mass separation among the Si and S fragments (cf. Fig. 2) and can see no way for us to have an excess of ^{32}S or ^{28}Si or any appreciable background. Note also that we are reporting data from three separate runs (three energies), each of which was analyzed separately and show comparable results for ^{32}S and ^{31}P.

While both experiments include corrections for secondary interactions in the target and instrument [5–8], it is possible that the differences in the experimental techniques used for these corrections might introduce a mass-dependent effect. Additional experimental work will be required to resolve this issue.

We can also compare our measurements to results from another earlier proton irradiation experiment that used natural calcium targets [33]. The two isotopes studied in that experiment, ^{22,24}Na, were found to have production cross sections of 0.34–1.2 mb for ^{24}Na and 0.61–2.6 mb for ^{22}Na in an energy range of 200–400 MeV/nucleon. These are in good agreement with the 356 MeV/nucleon values from this work of 0.5 ± 0.4 mb for ^{24}Na and 2.0 ± 0.7 mb for ^{22}Na, indicating no overproduction in our analysis.

Returning to the comparison with the predictive formulas (Fig. 6), for ^{34}S fragments both semiempirical and parametric predictions are very close and in agreement with our data, but both predictions fall short for ^{32}S. For ^{30}Si and ^{28}Si, the parametric predictions are somewhat closer to the data, but the energy dependence in the data is not reproduced by either model. For ^{26}Mg, however, the energy dependence is similar, but both predictions are below the measured values, while for ^{24}Mg the parametric calculation gives a good fit. On the other hand, both the semiempirical and the parametric predictions agree well with ^{20}Ne data and are very close for ^{22}Ne.

Figure 7 shows some of the dominant channels for odd-Z fragments. The overall picture is again similar to that of Fig. 6, with neither prediction able to match all the data. The agreement varies from being good with the parametric formulas (^{23}Na), to good with semiempirical (^{35}Cl), to bad for both (^{27}Al,^{31}P). Similar results are observed for other channels (not plotted). It is interesting that in some cases the semiempirical and/or parametric formulations are able to

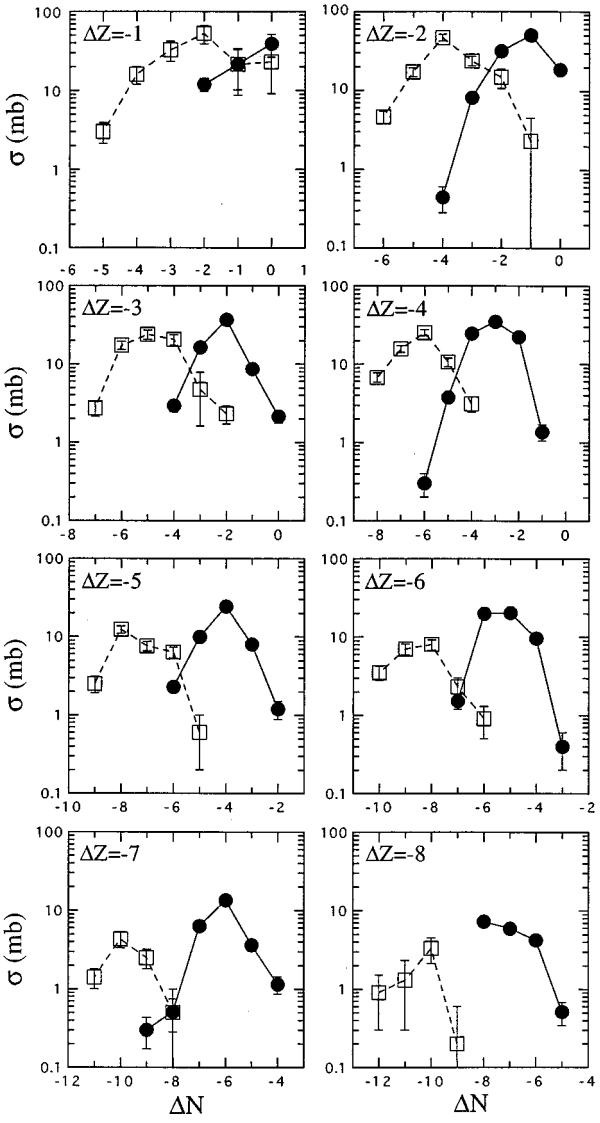

FIG. 4. Comparison between ^{40}Ca+H$\rightarrow X$ at 357 MeV/nucleon (solid circles) and ^{40}Ar+H$\rightarrow X$ at 352 MeV/nucleon (open squares). Isotopic production cross sections are plotted as a function of neutron change (ΔN) and grouped in proton change (ΔZ).

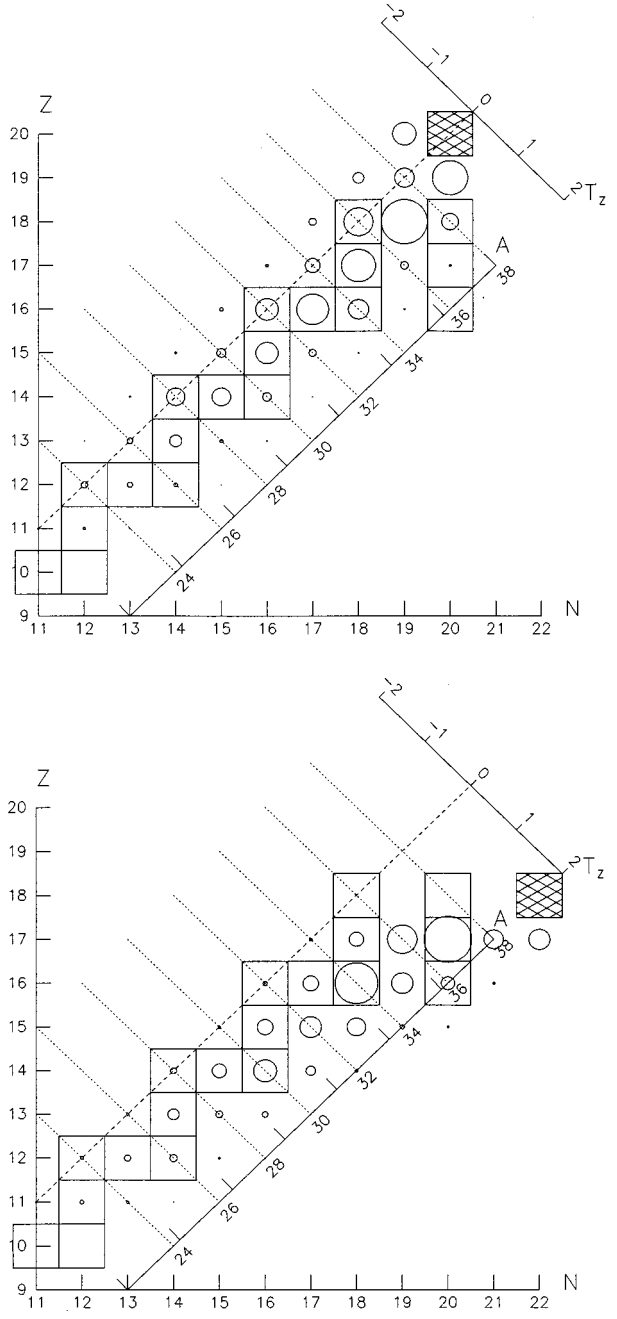

FIG. 5. Isotopic production cross section as a function of neutron (N) and proton (Z) numbers for ^{40}Ca+H$\rightarrow X$ at 357 MeV/nucleon (top) and ^{40}Ar+H$\rightarrow X$ at 352 MeV/nucleon (bottom). Open circles are cross section magnitude, with a diameter of one corresponding to 50 mb. Crosshatched squares are projectile nuclei. Open squares are stable nuclei. Also marked are total nuclear mass number (A) and nuclear isospin number (T_Z).

predict the measured energy dependence, but in many cases the dependence is quite different. These results imply that both cross section prediction techniques *may* need further revision if they are to be used for calculations of cosmic ray propagation through the ISM of new precision observations of GCR abundances that are now becoming available [34–37].

Such comparisons can lead to interesting astrophysical consequences. Some of the GCR source ratios, for example, ^{34}S/^{32}S, ^{30}Si/^{28}Si, and ^{29}Si/^{28}Si, are among the key differences separating the supermetallicity model from the Wolf-Rayet and *s*-process models [1–3], with the most recent GCR measurements indicating the solar system composition with the exception of ^{22}Ne/^{20}Ne [34–37]. The discrepancies between our cross section data and the predictions, e.g., the cases of ^{34}S and ^{32}S, can lead to significant impact upon the final astrophysical conclusions. The predicted secondary component of ^{34}S will not change appreciably since the data and the formulas are in substantial agreement. However, for ^{32}S the data from this work imply a ~30%–40% larger secondary contribution, while an earlier measurement [6] agrees with both predictions. This implies a lower ^{32}S source abundance and consequently a larger ^{34}S/^{32}S source ratio.

V. CONCLUSIONS

We report the measurement and the systematics of isotopic production cross sections from fragmentation of ^{40}Ca at

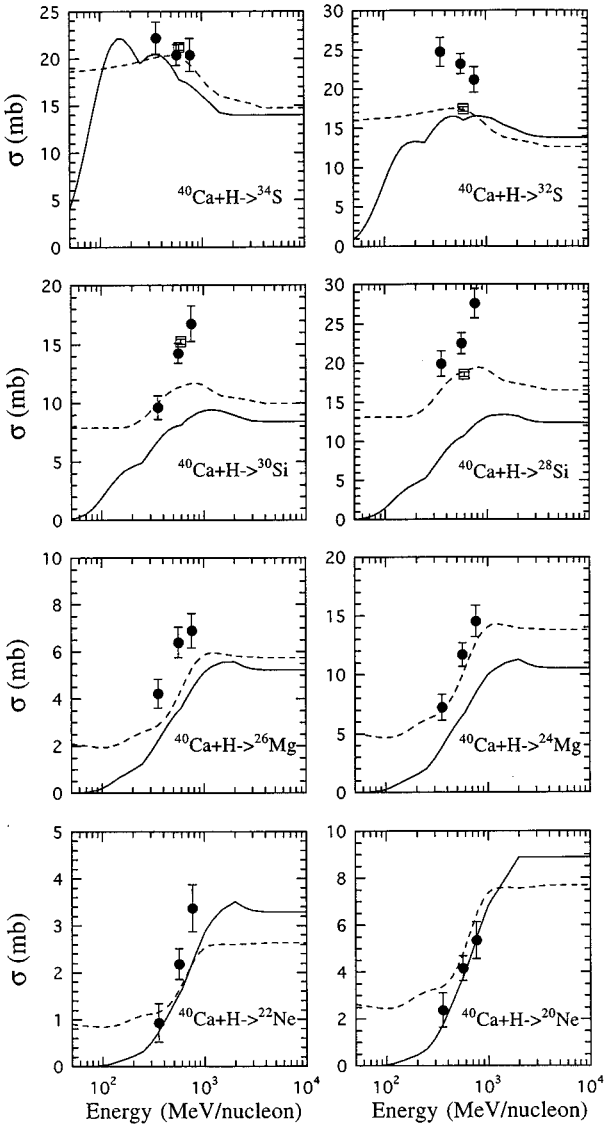

FIG. 6. Energy dependence of some even- Z fragments from ^{40}Ca+H$\rightarrow X$, solid circles are from this work. Open squares are previous data [6]. Solid curves are semiempirical predictions, and dashed curves are parametric predictions.

357, 565, and 763 MeV/nucleon in hydrogen. The results indicate that nuclear structure effects are present in the isotope production process during relativistic collisions. The new isotopic cross sections show various degrees of energy dependence not uniformly reproduced by any of the predictive techniques. Even though the projectile is a neutron-balanced species, the isotopic production overall favors neutron-rich fragments. Neither the Silberberg-Tsao semi-

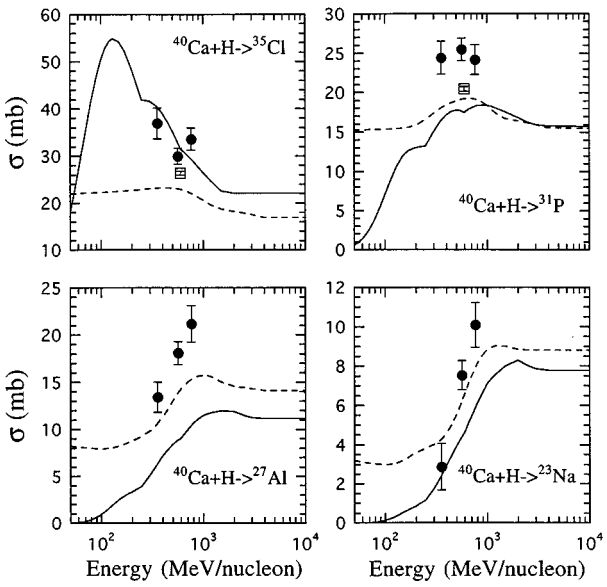

FIG. 7. Energy dependence of some odd-Z fragments from ^{40}Ca+H$\rightarrow X$. Solid circles are from this work. Open squares are previous data [6]. Solid curves are semiempirical predictions, and dashed curves are parametric predictions.

empirical cross section formulas [12] nor the Webber-Kish-Schrier parametric predictions fully describe these systematics [15]. The new cross data presented here can be utilized to refine the cross section prediction algorithms which are used to interpret cosmic ray observations of the abundances. Because of the lack of adequate heavy-ion facilities worldwide, future cosmic ray experiments will have to rely heavily upon cross section predictions. Therefore it is important to update the predictive formulas, using data such as those reported here, to ensure that the solutions to some astrophysical questions are not dominated by cross section inaccuracies.

ACKNOWLEDGMENTS

The Transport Collaboration thanks the LBL Bevalac staff for their support during the experiment. Thanks are also due to I. Flores, S. Ko, C. Kuo, and T. A. Murrell. Work supported at the Louisiana State University by NASA under Grant No. NAGW-1526 and by the U.S. DOE under Grant No. DE-FG05-ER 40147; at the University of California, Berkeley by NASA under Grant No. NGC 05-003-513; at the University of Minnesota by NASA under Grant No. NAGW-2004; at the Lawrence Berkeley Laboratory in part by NASA under Grant No. L14230C; at the New Mexico State University by NASA under Grant No. NAGW-3022; and at the Universita' di Catania, Italy by the INFN.

[1] J. P. Wefel, in *Genesis and Propagation of Cosmic Rays*, edited by M. M. Shapiro and J. P. Wefel, Vol. 220 of *NATO Advanced Study Institute, Series C* (Reidel, Dordrecht, 1988), p. 1.

[2] R. A. Mewaldt, in *Cosmic Abundances of Matter*, edited by C. J. Waddington, AIP Conf. Proc. No. 183 (AIP, New York, 1989), p. 124.

[3] J. P. Wefel, in *Cosmic Rays, Supernovae and the Interstellar Medium*, edited by M. M. Shapiro, R. Silberberg, and J. P. Wefel, Vol. 337 of *NATO Advanced Study Institute, Series C* (Kluwer, Dordrecht, 1991), p. 29.

[4] M. Garcia-Munoz, J. A. Simpson, T. G. Guzik, J. P. Wefel, and S. H. Margolis, Astrophys. J. Suppl. Ser. **64**, 269 (1987).

[5] W. R. Webber, J. C. Kish, and D. A. Schrier, Phys. Rev. C **41**, 533 (1990).

[6] W. R. Webber, J. C. Kish, and D. A. Schrier, Phys. Rev. C **41**, 547 (1990).

[7] C.-X. Chen, S. Albergo, Z. Caccia, S. Costa, H. J. Crawford, M. Cronqvist, J. Engelage, L. Greiner, T. G. Guzik, A. Insolia, C. N. Knott, P. J. Lindstrom, M. McMahon, J. W. Mitchell, R. Potenza, G. V. Russo, A. Soutoul, O. Testard, C. E. Tull, C. Tuvé, C. J. Waddington, W. R. Webber, and J. P. Wefel, Astrophys. J. **479**, 504 (1997).

[8] C. N. Knott, S. Albergo, Z. Caccia, C.-X. Chen, S. Costa, H. J. Crawford, M. Cronqvist, J. Engelage, P. Ferrando, R. Fonte, L. Greiner, T. G. Guzik, A. Insolia, F. C. Jones, P. J. Lindstrom, J. W. Mitchell, R. Potenza, J. Romanski, G. V. Russo, A. Soutoul, O. Testard, C. E. Tull, C. Tuvé, C. J. Waddington, W. R. Webber, and J. P. Wefel, Phys. Rev. C **53**, 347 (1996).

[9] C. E. Tull, S. Albergo, Z. Caccia, C.-X. Chen, S. Costa, H. J. Crawford, M. Cronqvist, J. Engelage, L. Greiner, T. G. Guzik, A. Insolia, C. N. Knott, P. J. Lindstrom, M. McMahon, J. W. Mitchell, R. Potenza, G. V. Russo, A. Soutoul, O. Testard, C. Tuvé, C. J. Waddington, W. R. Webber, and J. P. Wefel, in *Proceedings of the 23rd International Cosmic Ray Conference*, Calgary, Aberta, 1993, edited by D. A. Leahy, R. B. Hicks, and D. Venkatesan (World Scientific, Singapore, 1994), Vol. 2, p. 163.

[10] C. N. Knott, S. Albergo, Z. Caccia, C.-X. Chen, S. Costa, H. J. Crawford, M. Cronqvist, J. Engelage, L. Greiner, T. G. Guzik, A. Insolia, P. J. Lindstrom, J. W. Mitchell, R. Potenza, G. V. Russo, A. Soutoul, O. Testard, C. E. Tull, C. Tuvé, C. J. Waddington, W. R. Webber, and J. P. Wefel, Phys. Rev. C **56**, 398 (1997).

[11] R. Silberberg and C. H. Tsao, in *Proceedings of the 20th International Cosmic Ray Conference*, Moscow, 1987, edited by V. A. Kozyarivsky, A. S. Linvansky, T. I. Tulupova, A. L. Tsyabuk, A. V. Voevodsky, and N. S. Volgemut (Nauka, Moscow, 1987), Vol. 2, p. 133.

[12] R. Silberberg and C. H. Tsao, Phys. Rep. **191**, 351 (1990).

[13] L. Sihver, C. H. Tsao, R. Silberberg, T. Kanai, and A. F. Barghouty, Phys. Rev. C **47**, 1225 (1993).

[14] C. H. Tsao, R. Silberberg, A. F. Barghouty, L. Sihver, and T. Kanai, Phys. Rev. C **47**, 1257 (1993).

[15] W. R. Webber, J. C. Kish, and D. A. Schrier, Phys. Rev. C **41**, 566 (1990).

[16] G. Crinklaw and S. R. Federman, Astrophys. J. **424**, 748 (1994).

[17] S. E. Woosley and T. A. Weaver, Astrophys. J. Suppl. Ser. **101**, 181 (1995).

[18] N. Prantzos, M. Arnould, and J.-P. Arcoragi, Astrophys. J. **315**, 209 (1987).

[19] A. G. W. Cameron, P. Höflich, P. C. Myers, and D. D. Clayton, Astrophys. J. **447**, L53 (1995).

[20] G. J. Wasserburg, M. Busso, and R. Gallino, Astrophys. J. **466**, L109 (1996).

[21] S. Amari, E. Zinner, and R. S. Lewis, Astrophys. J. **447**, L147 (1995).

[22] S. Amari, E. Zinner, and R. S. Lewis, Astrophys. J. **470**, L101 (1996).

[23] S. T. Hsieh, M. C. Wang, and D. S. Chuu, Phys. Rev. C **23**, 521 (1981).

[24] A. Andl, K. Bekk, S. Göring, A. Hanser, G. Nowicki, H. Rebel, G. Schatz, and R. C. Thompson, Phys. Rev. C **26**, 2194 (1982).

[25] H. D. Wohlfahrt, E. B. Shera, and M. V. Hoehn, Phys. Rev. C **23**, 533 (1983).

[26] G. Shanmugam and M. Thiagasundaram, Phys. Rev. C **39**, 1623 (1989).

[27] L. Vermeerent, P. Lievens, R. E. Silverans, U. Georg, M. Keim, A. Klein, R. Neugart, M. Neuroth, F. Buchinger, and the ISOLDE Collaboration, J. Geophys. Res. **22**, 1517 (1996).

[28] T. G. Guzik, S. Albergo, Z. Caccia, C.-X. Chen, S. Costa, H. J. Crawford, J. Engelage, P. Ferrando, I. Flores, L. Greiner, F. C. Jones, C. N. Knott, S. Ko, P. J. Lindstrom, J. Mazotta, J. W. Mitchell, R. Potenza, J. Romanski, G. V. Russo, A. Soutoul, O. Testard, C. E. Tull, C. Tuvé, C. J. Waddington, W. R. Webber, J. P. Wefel, and X. Zhang, Adv. Space Res. **14**, 825 (1994).

[29] C.-X. Chen, S. Albergo, Z. Caccia, S. Costa, H. J. Crawford, M. Cronqvist, J. Engelage, P. Ferrando, R. Fonte, L. Greiner, T. G. Guzik, A. Insolia, F. C. Jones, C. N. Knott, P. J. Lindstrom, J. W. Mitchell, R. Potenza, J. Romanski, G. V. Russo, A. Soutoul, O. Testard, C. E. Tull, C. Tuvé, C. J. Waddington, W. R. Webber, J. P. Wefel, and X. Zhang, Phys. Rev. C **49**, 3200 (1994).

[30] J. Engelage, S. Albergo, C.-X. Chen, S. Costa, H. J. Crawford, P. Ferrando, L. Greiner, T. G. Guzik, F. C. Jones, C. N. Knott, S. Ko, C. Kuo, P. J. Lindstrom, U. Lynen, J. Mazotta, J. W. Mitchell, W. F. J. Mueller, D. Olson, R. Potenza, A. Soutoul, T. J. M. Symons, O. Testard, C. E. Tull, C. Tuvé, C. J. Waddington, W. R. Webber, J. P. Wefel, and H. H. Wieman, in *Proceedings of the 22nd International Cosmic Ray Conference* Dublin, edited by M. Cawley, L. O'C. Drury, D. J. Fegan, D. O'Sullivan, N. A. Porter, J. J. Quenby, and A. A. Watsen (Dublin Institute for Advanced Studies, Dublin, 1991), Vol. 2, p. 531.

[31] S. Albergo, Z. Caccia, C.-X. Chen, S. Costa, H. J. Crawford, M. Cronqvist, J. Engelage, I. Flores, R. Fonte, L. Greiner, T. G. Guzik, A. Insolia, C. N. Knott, S. Ko, C. Kuo, P. J. Lindstrom, J. Mazotta, M. McMahon, J. W. Mitchell, R. Potenza, J. Romanski, G. V. Russo, A. Soutoul, O. Testard, C. E. Tull, C. Tuvé, C. J. Waddington, W. R. Webber, and J. P. Wefel, Radiat. Meas. (to be published).

[32] C. Tuvé, S. Albergo, D. Boemi, Z. Caccia, C.-X. Chen, S. Costa, H. J. Crawford, M. Cronqvist, J. Engelage, L. Greiner, T. G. Guzik, A. Insolia, C. N. Knott, P. J. Lindstrom, J. W. Mitchell, R. Potenza, S. Rieto, J. Romanski, G. V. Russo, A. Soutoul, O. Testard, C. E. Tull, C. J. Waddington, W. R. Webber, and J. P. Wefel, Phys. Rev. C **56**, 1057 (1997).

[33] R. G. Korteling and A. A. Caretto, Jr., Phys. Rev. C **1**, 1960 (1970).

[34] J. J. Connell and J. A. Simpson, in *Proceedings of the 23rd International Cosmic Ray Conference* [9], Vol. 1, p. 559.

[35] M. A. DuVernois, M. Garcia-Munoz, F. R. Pyle, and J. A. Simpson, in *Proceedings of the 23rd International Cosmic Ray Conference* [9], Vol. 1, p. 563.

[36] A. Hesse, B. S. Acharya, U. Heinbach, W. Heinrich, M. Henkel, B. Luzietti, M. Simon, U. K. Balasubrahmanyan, L. M. Barbier, E. R. Christian, J. A. Esposito, J. F. Ormes, and R. E. Streitmatter, in Proceedings of the 23rd International Cosmic Ray Conference [9], Vol. 1, p. 567.

[37] M. R. Thayer, in *Proceedings of the 24th International Cosmic Ray Conference*, Rome, 1995, edited by N. Iucci and E. Lamanna (Societa Italiana di Fisica, Editrice Compositori, Bologna, Italy, 1996), Vol. 3, p. 124..